

Distributed Consensus-Based Demodulation: Algorithms and Error Analysis

Hao Zhu, *Student Member, IEEE*, Alfonso Cano, *Student Member, IEEE*,
and Georgios B. Giannakis, *Fellow, IEEE*

Abstract—This paper deals with distributed demodulation of space-time transmissions of a common message from a multi-antenna access point (AP) to a wireless sensor network. Based on local message exchanges with single-hop neighboring sensors, two algorithms are developed for distributed demodulation. In the first algorithm, sensors consent on the estimated symbols. By relaxing the finite-alphabet constraints on the symbols, the demodulation task is formulated as a distributed convex optimization problem that is solved iteratively using the method of multipliers. Distributed versions of the centralized zero-forcing (ZF) and minimum mean-square error (MMSE) demodulators follow as special cases. In the second algorithm, sensors iteratively reach consensus on the average (cross-) covariances of locally available per-sensor data vectors with the corresponding AP-to-sensor channel matrices, which constitute sufficient statistics for maximum likelihood demodulation. Distributed versions of the sphere decoding algorithm and the ZF/MMSE demodulators are also developed. These algorithms offer distinct merits in terms of error performance and resilience to non-ideal inter-sensor links. In both cases, the per-iteration error performance is analyzed, and the approximate number of iterations needed to attain a prescribed error rate are quantified. Simulated tests verify the analytical claims. Interestingly, only a few consensus iterations (roughly as many as the number of sensors), suffice for the distributed demodulators to approach the performance of their centralized counterparts.

Index Terms—Detection and estimation, sensor networks, cooperative diversity.

I. INTRODUCTION

OVER the last years, there has been an increasing interest in wireless cooperative communications [2], [3]. In the cooperative broadcast scenario, all users are interested in the common message sent, but may not have sufficient signal quality to individually determine the message - a case motivating well the need for cooperation. This scenario emerges naturally in applications involving wireless sensor networks (WSNs). Consider a group of resource-constrained sensors wishing to demodulate a common message broadcast from an access point (AP). For efficiency reasons, the AP transmits

only limited redundant information and/or the sensors cannot request retransmissions when errors are detected. For instance, the AP might be an unmanned aerial vehicle (UAV) flying over a WSN deployed on the ground, and broadcasting lasts for only a short period of time. Moreover, due to limited resources, sensors may only afford linear demodulation modules. In such cases, collaboration among sensors is imperative to improve the quality of locally received information. Furthermore, due to communication and energy constraints, inter-sensor communications may be restricted to one-hop transmissions. In this context, the objective of this paper is to develop distributed algorithms to demodulate a common space-time matrix transmitted from a multi-antenna AP.

From an information-theoretic perspective, the problem of interactive decoding of a common message over a broadcast channel was studied in [3], [2], [10] and references therein. Limited to a pair of users, these works seek the optimal number of conversation rounds [3] or the achievable capacity region [2], [10]. Hierarchical modulations were explored for broadcasting to a set of uneven quality destinations, followed by successive broadcasts by some of the destinations [17]. From a signal processing viewpoint, various distributed algorithms have been developed to exploit collaboration among neighboring sensors for detection-estimation problems, mostly through iterative exchanges of information-bearing messages. The specific problem of distributed consensus averaging (CA) of data collected across sensors has been considered in many works; see e.g., [7], [13], [18] and references thereof. A general algorithm for distributed parameter estimation [15] is also available using the method of multipliers (MoM) [1, Sec.3.4.4]. Distributed hypotheses testing (DHT) approaches, whereby sensors agree on the optimal hypothesis using either CA or belief propagation can be found in [8], [11] and [14].

Pursuing the implications these CA-MoM ideas have for wireless communications, the present paper develops two algorithms for solving *distributed* demodulation and equalization problems, using: (a) distributed consensus on demodulated symbol (DC-DS) estimates; and (b) distributed consensus on sufficient statistics (DC-SS). In the DC-DS approach, the centralized zero-forcing (ZF) and minimum mean-square error (MMSE) demodulators are reformulated as a convex optimization problem that is solved iteratively in a distributed fashion using the MoM. An analytical approximation to the symbol error rate (SER) per iteration of the algorithm is also derived. In the DC-SS algorithm, on the other hand, sensors iteratively reach network-wide consensus on the average of sample (cross-) covariances of locally available per-sensor data vectors with the AP-to-sensor channel matrix, which constitute sufficient statistics for maximum likelihood (ML)

Manuscript received June 12, 2009; revised December 2, 2009; accepted February 23, 2010. The associate editor coordinating the review of this paper and approving it for publication was M. Valenti.

This work was supported by NSF grants CCF 0830480 and CON 014658; and also through collaborative participation in the Communications and Networks Consortium sponsored by the U.S. Army Research Laboratory under the Collaborative Technology Alliance Program, Cooperative Agreement DAAD19-01-2-0011. The U.S. Government is authorized to reproduce and distribute reprints for Government purposes notwithstanding any copyright notation therein. Part of this work was presented at the 42nd Asilomar Conference on Signals, Systems, and Computers, Pacific Grove, CA, Oct. 2008.

The authors are with the Department of Electrical and Computer Engineering, University of Minnesota, 200 Union Street SE, Minneapolis, MN 55455 USA (e-mail: {zhuh, alfonso, georgios}@umn.edu).

Digital Object Identifier 10.1109/TWC.2010.06.090890

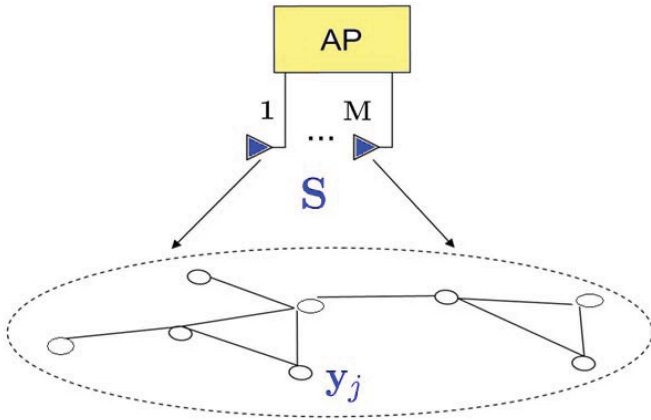


Fig. 1. System model.

demodulation. Upon obtaining sufficient statistics per sensor it becomes possible to perform general (possibly non-linear) demodulation, including distributed sphere decoding (SD) and ZF/MMSE demodulation. Per-iteration pairwise error probability (PEP) bounds of the ML demodulator are included, establishing that full diversity is achieved in a finite number of iterations. An analytical approximation to the SER per iteration for linear demodulators is also provided. Compared to related DHT algorithms [8], [11], [14], both DC-DS and DC-SS can afford reduced overhead in inter-sensor communications, irrespective of the number of hypotheses, which is exponential in the dimensionality of the space-time matrix, and the number of bits per constellation symbol. Compared to [19], which deals with consensus-based hard and soft channel decoding, the present work offers linear demodulators (with corresponding error analysis), and diversity analysis for ML demodulators. Simulated tests demonstrate faster convergence for the DC-SS under ideal inter-sensor links, while the DC-DS offers robustness to non-ideal links.

The rest of the paper is organized as follows. In Section II, the system model is introduced and the distributed ML demodulation problem is formulated. The DC-DS algorithm is developed in Section III along with expressions for the SER per iteration. The DC-SS algorithm and its SER analysis per iteration are the subjects of Section IV. Simulations corroborating the analytical findings are provided in Section V.

Notation: Upper (lower) bold face letters are used for matrices (column vectors); $\text{vec}(\mathbf{X})$ is a vector formed by concatenating the columns of \mathbf{X} ; \otimes stands for the Kronecker product; $(\cdot)^T$ denotes transposition; \mathbf{I}_N the $N \times N$ identity matrix; $\mathbf{1}_N$ the $N \times 1$ vector of all-ones; $\mathbf{0}_N$ the $N \times 1$ all-zero vector; $\|\cdot\|$ the Frobenius norm; $|\cdot|$ the cardinality of a set; and $\mathcal{N}(\mu, \sigma^2)$ the Gaussian distribution with mean μ and variance σ^2 .

II. MODELING AND PROBLEM STATEMENT

Consider a (possibly mobile) access point (AP) equipped with M antennas as depicted in Fig. 1. Constellation symbols at the AP are mapped to an $M \times N$ space-time matrix \mathbf{S} belonging to a finite alphabet \mathcal{A} , where N is the number of time slots. The AP broadcasts \mathbf{S} to a connected *ad hoc* WSN with J single-antenna sensors. The WSN is modeled as

a graph $\mathcal{G} := \{\mathcal{E}, \mathcal{J}\}$, where $\mathcal{J} := \{1, \dots, J\}$ denotes the set of sensors, and $\mathcal{E} \subset \mathcal{J} \times \mathcal{J}$ the set of available communication links (graph edges). The set of neighbors of sensor j is denoted by $\mathcal{N}_j \subseteq \mathcal{J}$. The following is assumed regarding connectivity of sensors.

(as1) The WSN is connected; i.e., there is a (possibly multi-hop) path connecting any two nodes; in addition, all inter-sensor links are ideal, and time-invariant per-block.

Note that \mathcal{G} can contain cycles. Ideal (virtually error-free) inter-sensor communications are possible with sufficiently fine quantization and powerful error control codes. However, the subsequent analysis can be modified to accommodate imperfect sensor links corrupted by additive zero-mean noise and/or random link failures as in [19]; see also simulated tests in Section V.

With reference to Fig. 1, the $N \times 1$ received block \mathbf{y}_j at the j -th sensor is given by the following input/output (I/O) relationship

$$\mathbf{y}_j = \mathbf{S}^T \mathbf{h}_j + \epsilon_j \quad (1)$$

where \mathbf{h}_j denotes the $M \times 1$ AP-to-sensor j fading channel, and $\epsilon_j \sim \mathcal{N}(\mathbf{0}_N, \mathbf{I}_N)$ stands for additive white Gaussian noise (AWGN) that is assumed uncorrelated across sensors. By properly scaling \mathbf{y}_j , the noise ϵ_j can be assumed without loss of generality (wlog) to have zero mean and unit variance. The following is assumed regarding the AP-to-sensor channels.

(as2) The fading coefficients \mathbf{h}_j between the AP and sensor j remain static over the AP-to-sensor transmission time, but are allowed to change from transmission to transmission. Each sensor j acquires \mathbf{h}_j through training.

With the definitions $\mathbf{H}_j := \mathbf{I}_N \otimes \mathbf{h}_j^T$ and $\mathbf{s} := \text{vec}(\mathbf{S})$, the I/O relationship in (1) can be rewritten as $\mathbf{y}_j = \mathbf{H}_j \mathbf{s} + \epsilon_j$. And with $\mathbf{y} := [\mathbf{y}_1^T, \dots, \mathbf{y}_J^T]^T$ collecting the received blocks across sensors, the $NJ \times 1$ vector \mathbf{y} can be compactly expressed as

$$\mathbf{y} = \mathbf{H} \mathbf{s} + \epsilon \quad (2)$$

where $\mathbf{H} := [\mathbf{H}_1^T, \dots, \mathbf{H}_J^T]^T$, and $\epsilon := [\epsilon_1^T, \dots, \epsilon_J^T]^T$. For notational brevity, but also wlog, focus will be placed on real baseband equivalent models instead of complex ones. The complex case can be accommodated either by working directly with a complex model, or, through a real-equivalent model having twice the dimension of the complex one; see e.g [4, Sec 5.1].

(as3) Symbols in \mathbf{s} are independently and uniformly drawn from alphabet \mathcal{A} , that is known to all sensors.

Note that (as3) allows even for space-time coded transmissions. In this case, \mathbf{H} denotes an equivalent channel matrix combining the physical channel with the underlying linear constellation precoding or an orthogonal space-time block code matrix [4, Ch. 3.3, 3.5].

Given (as2) and (as3), and since the noise ϵ has uncorrelated entries of equal variance, the *centralized* ML demodulator for (2) amounts to finding

$$\begin{aligned} \hat{\mathbf{s}}_{ML} &= \arg \max_{\mathbf{s} \in \mathcal{A}^{NM}} -\|\mathbf{y} - \mathbf{H} \mathbf{s}\|^2 \\ &= \arg \max_{\mathbf{s} \in \mathcal{A}^{NM}} -\sum_{j=1}^J \|\mathbf{y}_j - \mathbf{H}_j \mathbf{s}\|^2. \end{aligned} \quad (3)$$

Clearly, if $\{\mathbf{y}_j, \mathbf{H}_j\}_{j=1}^J$ were available at a central location (or at all sensors), then $\hat{\mathbf{s}}_{ML}$ in (3) could be centrally (locally) found. However, $\{\mathbf{y}_j, \mathbf{H}_j\}_{j=1}^J$ are distributed across the network. The objective of this paper is to find suitable single-hop inter-sensor exchanges such that each sensor is able to solve the centralized demodulation problem (or a relaxed version thereof) in a *distributed* fashion.

Remark 1. (*Comparison with DHT problems*) The centralized ML demodulation problem in (3) can be viewed as a multiple hypotheses testing problem, where each hypothesis is a block \mathbf{S} with entries drawn from \mathcal{A} . Therefore, this problem can in principle be solved by the DHT algorithms developed for sensor networks in e.g., [8], [11], and [14]. However, these schemes - designed primarily for detection problems entailing a few hypotheses - require implementation of a distributed algorithm for each hypothesis. When it comes to demodulating wireless transmissions, their complexity grows exponentially with the number of bits per constellation symbol and, for the present space-time broadcast setup, with the product NM . Using knowledge of the alphabet and the modulation scheme, the distinct contribution of this paper is twofold: a) reduce the complexity of the DHT algorithms in [8], [11], [14]; and b) provide thorough error analysis for distributed demodulation and equalization. These tasks were not addressed in our companion paper [19], which dealt with consensus-based hard and soft channel decoding (as opposed to demodulation).

III. DISTRIBUTED LINEAR DEMODULATORS

This section introduces a linear distributed demodulation algorithm for solving (3). To this end, the centralized linear demodulation task is formulated as a convex optimization problem that can be distributed across sensors. Two popular linear demodulators will be considered jointly: the zero-forcing (ZF) and the minimum mean-square error (MMSE) demodulators [12, Ch. 10.2]. The ZF one inverts the channel effects by multiplying the received signal vector in (2) by the pseudo-inverse of the channel matrix [4, Eq. (5.3)]. It can be seen as the solution of an unconstrained least-squares problem [cf. (3)]

$$\hat{\mathbf{s}}_{ZF} = \arg \min_{\mathbf{s}} \frac{1}{2} \sum_{j=1}^J \|\mathbf{y}_j - \mathbf{H}_j \mathbf{s}\|^2 = (\mathbf{H}^T \mathbf{H})^{-1} \mathbf{H}^T \mathbf{y}. \quad (4)$$

Different from (3), where \mathbf{s} is drawn from the finite-alphabet (constellation) \mathcal{A}^{NM} , the minimization in (4) does not constrain \mathbf{s} . The centralized MMSE demodulator, namely $\hat{\mathbf{s}}_{MMSE} = E\{\mathbf{s}\mathbf{y}^T\}E^{-1}\{\mathbf{y}\mathbf{y}^T\}\mathbf{y}$, can also be expressed in closed form as

$$\begin{aligned} \hat{\mathbf{s}}_{MMSE} &= \sigma_s^2 \mathbf{H}^T (\sigma_s^2 \mathbf{H} \mathbf{H}^T + \mathbf{I}_{NJ})^{-1} \mathbf{y} \\ &= (\mathbf{H}^T \mathbf{H} + \sigma_s^{-2} \mathbf{I}_{NM})^{-1} \mathbf{H}^T \mathbf{y} \end{aligned} \quad (5)$$

where $\sigma_s^2 := E\{s_\ell^2\}$, $\ell = 1, \dots, NM$ denotes the average symbol energy; and the second equality comes from the matrix inversion lemma. Similar to the ZF demodulator, (5) can be viewed as the solution of an unconstrained LS problem as

follows

$$\begin{aligned} \hat{\mathbf{s}}_{MMSE} &= \left(\sum_{j=1}^J \mathbf{H}_j^T \mathbf{H}_j + \sigma_s^{-2} \mathbf{I}_{NM} \right)^{-1} \left(\sum_{j=1}^J \mathbf{H}_j^T \mathbf{y}_j \right) \\ &= \arg \min_{\mathbf{s}} \frac{1}{2} \sum_{j=1}^J \|\mathbf{y}'_j - \mathbf{H}'_j \mathbf{s}\|^2 \end{aligned} \quad (6)$$

where $\mathbf{H}'_j := [\mathbf{H}_j^T, (\sigma_s \sqrt{J})^{-1} \mathbf{I}_{NM}]^T$, and $\mathbf{y}'_j := [\mathbf{y}_j^T, \mathbf{0}_{NM}^T]^T$.

Equation (6) shows that the centralized MMSE demodulator is obtained from an LS minimization problem similar to the one in (4). Hence, all the ensuing results developed for distributed ZF demodulators carry over to the MMSE ones, by simply substituting \mathbf{H}'_j for \mathbf{H}_j , and \mathbf{y}'_j for \mathbf{y}_j .

A. Distributed Consensus on Demodulated Symbols

The objective of this section is to solve to (4) in a distributed fashion through message exchanges among single-hop neighboring sensors. This task will be accomplished using the method of multipliers (MoM) [1, Sec. 3.4.4]. The MoM can afford distributed implementation through *local auxiliary* variables \mathbf{s}_j , which represent the wanted ZF solution per sensor j . Let $\mathbf{s} := \{\mathbf{s}_j\}_{j=1}^J$ be a set of all these J auxiliary variables, one per sensor. (Notice that the set \mathbf{s} is different from the transmitted vector \mathbf{s} in (2).) The set \mathbf{s} can be obtained by minimizing the following consensus-constrained quadratic cost function

$$\begin{aligned} \min_{\mathbf{s}} \quad & \frac{1}{2} \sum_{j=1}^J \|\mathbf{y}_j - \mathbf{H}_j \mathbf{s}_j\|^2 \\ \text{s.t.} \quad & \mathbf{s}_j - \mathbf{s}_i = \mathbf{0}_{NM}, \quad j \in \mathcal{J}, i \in \mathcal{N}_j. \end{aligned} \quad (7)$$

Thanks to \mathbf{s}_j , the sum-cost can be decoupled, and each summand can be minimized separately per sensor j . On the other hand, the neighborhood consensus constraint in (7) ensures that consensus is achieved over the entire network, which was assumed connected. Network connectivity provides a sufficient condition to guarantee that the optimum of (7) per sensor j satisfies $\mathbf{s}_1 = \mathbf{s}_2 = \dots = \mathbf{s}_J = \hat{\mathbf{s}}_{ZF}$, where $\hat{\mathbf{s}}_{ZF}$ is the solution of (4).

After introducing an additional set of variables $\mathbf{z} := \{\{\mathbf{z}_{ji}, \mathbf{z}'_{ji}\}_{i \in \mathcal{N}_j}\}_{j \in \mathcal{J}}$, the problem (7) can be equivalently written as

$$\begin{aligned} \min_{\mathbf{s}, \mathbf{z}} \quad & \frac{1}{2} \sum_{j=1}^J \|\mathbf{y}_j - \mathbf{H}_j \mathbf{s}_j\|^2 \\ \text{s.t.} \quad & \mathbf{s}_j - \mathbf{z}_{ji} = \mathbf{0}_{NM}, \quad \mathbf{s}_i + \mathbf{z}'_{ji} = \mathbf{0}_{NM}, \\ & \mathbf{z}_{ji} + \mathbf{z}'_{ji} = \mathbf{0}_{NM} \quad j \in \mathcal{J}, i \in \mathcal{N}_j \end{aligned} \quad (8)$$

Let \mathbf{v}_{ji} and \mathbf{v}'_{ji} denote the Lagrange multipliers associated with the constraints $\mathbf{s}_j - \mathbf{z}_{ji} = \mathbf{0}_{NM}$ and $\mathbf{s}_i + \mathbf{z}'_{ji} = \mathbf{0}_{NM}$, respectively. Likewise, define the set $\mathcal{C}_z := \{\mathbf{z} : \mathbf{z}_{ji} + \mathbf{z}'_{ji} = \mathbf{0}_{NM}, \forall j \in \mathcal{J}, i \in \mathcal{N}_j\}$ that represents the constraints on the entries of \mathbf{z} . With $\alpha > 0$ denoting a penalty coefficient,

consider the augmented Lagrangian function of (8), namely

$$\begin{aligned} \mathcal{L}_a(\mathbf{s}, \mathbf{z}, \mathbf{v}, \mathbf{v}') = & \frac{1}{2} \sum_{j=1}^J \|\mathbf{y}_j - \mathbf{H}_j \mathbf{s}_j\|^2 \\ & + \sum_{j=1}^J \sum_{i \in \mathcal{N}_j} \{ \mathbf{v}_{ji}^T (\mathbf{s}_j - \mathbf{z}_{ji}) + (\mathbf{v}'_{ji})^T (-\mathbf{s}_i - \mathbf{z}'_{ji}) \} \\ & + \frac{\alpha}{2} \sum_{j=1}^J \sum_{i \in \mathcal{N}_j} \{ \|\mathbf{s}_j - \mathbf{z}_{ji}\|^2 + \|-\mathbf{s}_i - \mathbf{z}'_{ji}\|^2 \} \end{aligned} \quad (9)$$

where the set $\mathbf{v} := \{ \{ \mathbf{v}_{ji} \}_{i \in \mathcal{N}_j} \}_{j \in \mathcal{J}}$, and likewise for \mathbf{v}' .

The alternating-direction MoM operates by minimizing \mathcal{L}_a in (9) cyclically with respect to (w.r.t.) one set of variables given the other variables, considering the constraint set \mathcal{C}_z . Appendix A shows that under proper initialization, the variables \mathbf{v}' and $\{ \{ \mathbf{z}'_{ji} \}_{i \in \mathcal{N}_j} \}_{j \in \mathcal{J}}$ can be eliminated, and the k -th iteration of the MoM solver becomes

$$\mathbf{v}_{ji}(k) = \mathbf{v}_{ji}(k-1) + \frac{\alpha}{2} (\mathbf{s}_j(k) - \mathbf{s}_i(k)), \quad j \in \mathcal{J}, i \in \mathcal{N}_j \quad (10a)$$

$$\begin{aligned} \mathbf{s}_j(k+1) = & (\mathbf{H}_j^T \mathbf{H}_j + 2\alpha |\mathcal{N}_j| \mathbf{I}_{NM})^{-1} \left\{ \mathbf{H}_j^T \mathbf{y}_j - \sum_{i \in \mathcal{N}_j} [\mathbf{v}_{ji}(k) \right. \\ & \left. - \mathbf{v}_{ij}(k) - \alpha (\mathbf{s}_j(k) + \mathbf{s}_i(k))] \right\}, \quad j \in \mathcal{J}. \end{aligned} \quad (10b)$$

Iterations (10a) and (10b) constitute the DC-DS algorithm. Sensor $j \in \mathcal{J}$ maintains the local estimate of the ZF solution $\mathbf{s}_j(k)$ and all the multipliers $\{ \mathbf{v}_{ji}(k) \}_{i \in \mathcal{N}_j}$. During the k -th iteration, sensor j receives the broadcasted estimates $\mathbf{s}_i(k)$ from all its neighboring sensors $i \in \mathcal{N}_j$, and updates the corresponding multipliers via (10a). It then transmits back the updated multiplier $\mathbf{v}_{ji}(k)$ to each of its neighboring sensors $i \in \mathcal{N}_j$, based on which each sensor j is able to determine $\mathbf{s}_j(k+1)$ via (10b). Subsequently, all sensors $j \in \mathcal{J}$ broadcast their updated estimates $\mathbf{s}_j(k+1)$ to their neighbors, thus completing the k -th iteration and initializing the next one.

Notice that the overall number of scalars required to consent on is NM , regardless of the number of hypotheses $|\mathcal{A}|^{NM}$. This presents considerable communication savings compared to the DHT solvers of (3) in [11] and [14]. Equally important, the iterates in (10a)-(10b) are provably convergent, as asserted in the following proposition.

Proposition 1. (*DC-DS with ideal inter-sensor links*) *The iterations (10a) and (10b) with arbitrary initialization of $\mathbf{s}_j(1)$ and $\mathbf{v}_{ji}(0)$, $\forall (j, i) \in \mathcal{E}$ and $\alpha > 0$, reach consensus to the centralized ZF demodulation $\hat{\mathbf{s}}_{ZF}$ in (4) as $k \rightarrow \infty$; i.e.,*

$$\lim_{k \rightarrow \infty} \mathbf{s}_j(k) = \hat{\mathbf{s}}_{ZF}, \quad \forall j \in \mathcal{J}. \quad (11)$$

Proof: Appendix A shows that iterations (10a)-(10b) are equivalent to the MoM approach in [1, pg. 255]. As the cost function in (8) is convex and the problem constraints comply with [1, Assumption 4.1, pg. 255], the iterates converge to the optimal solution to (8) as established by [1, Prop. 4.2, pg. 256]. ■

Remark 2. (*Imperfect inter-sensor links*) Supposing that sufficiently powerful error control codes are employed, the inter-sensor messages involved in the DC-DS iterations have been so far assumed ideal; i.e., local exchanges are received error free. However, (10a) and (10b) can be modified to also accommodate inter-sensor links that fail randomly and/or have noise added at the receiving end [19]. Random link failures model severe fading or receiver noise for which the cyclic redundancy check (CRC) code detects and discards packets as erroneous. Whether analog or digital modulation is used, the additive noise present in the inter-sensor links can model Gaussian thermal noise at the receiver and/or (e.g., uniformly distributed) quantization noise. Mimicking [19], it can be shown that if the inter-sensor links are corrupted with additive noise, the DC-DS will converge in the mean, i.e., $\lim_{k \rightarrow \infty} E\{\mathbf{s}_j(k) - \hat{\mathbf{s}}_{ZF}\} = \mathbf{0}_{NM}$, with a bounded variance. Finally, if the inter-sensor links fail randomly and the failures follow a Bernoulli process, then DC-DS will converge in the mean-square sense (m.s.s.); i.e., $\lim_{k \rightarrow \infty} E\{\|\mathbf{s}_j(k) - \hat{\mathbf{s}}_{ZF}\|^2\} = 0$.

Remark 3. (*Comparison with [15]*) The DC-DS algorithm of this section is related to the consensus-based distributed best linear unbiased estimators in [15]. Compared to [15], the algorithm here offers three distinct novelties: (i) it does not require a bridge sensor set with which sensors need to communicate, thus offering a *fully* distributed approach; (ii) it is provably convergent in the presence of inter-sensor link failures; and (iii) it is possible to analyze the error performance per iteration, which is the topic of the next subsection.

B. Performance Analysis

The key to evaluating error performance per iteration k is to specify the relationship between $\mathbf{s}_j(k)$ and \mathbf{s} as a function of k . To this end, the following lemma is instrumental.

Lemma 1. *The consensus-based ZF iterates in (10a)-(10b) can be expressed as the linear superposition*

$$\mathbf{s}_j(k) = \sum_{i=1}^J \mathbf{C}_{ji}(k) \mathbf{y}_i, \quad \forall j \in \mathcal{J} \quad (12)$$

where the coefficient matrix $\mathbf{C}_{ji}(k)$ depends solely on the network topology and α .

Proof: See Appendix B. ■

Using (12) into (11), Proposition 1 and (4) imply that $\lim_{k \rightarrow \infty} \mathbf{C}_{ji}(k) = (\mathbf{H}^T \mathbf{H})^{-1} \mathbf{H}_j^T$, $\forall j$. Substituting \mathbf{y}_i from (1) into (12), it is further possible to express $\mathbf{s}_j(k)$ as

$$\mathbf{s}_j(k) = \mathbf{G}_j(k) \mathbf{s} + \mathbf{w}_j(k) \quad (13)$$

where $\mathbf{G}_j(k)$ and $\mathbf{w}_j(k)$ are defined, respectively, as

$$\mathbf{G}_j(k) := \sum_{i=1}^J \mathbf{C}_{ji}(k) \mathbf{H}_i, \quad \text{and} \quad \mathbf{w}_j(k) := \sum_{i=1}^J \mathbf{C}_{ji}(k) \boldsymbol{\epsilon}_i. \quad (14)$$

Vector $\mathbf{w}_j(k)$ denotes zero-mean colored Gaussian noise with covariance matrix $\boldsymbol{\Sigma}_j(k) := \sum_{i=1}^J \mathbf{C}_{ji}(k) \mathbf{C}_{ji}^T(k)$. Using these definitions, the ℓ -th entry of $\mathbf{s}_j(k)$ satisfies (cf. (13))

$$s_{j,\ell}(k) = g_{j,\ell\ell}(k) s_\ell + \sum_{\substack{\ell'=1 \\ \ell' \neq \ell}}^{NM} g_{j,\ell\ell'}(k) s_{\ell'} + w_{j,\ell}(k) \quad (15)$$

where $g_{j,\ell\ell'}(k)$ and $w_{j,\ell}(k)$ are the (ℓ, ℓ') -th and ℓ -th entries of $\mathbf{G}_j(k)$ and $\mathbf{w}_j(k)$, respectively. The last two terms in the right-hand side of (15) capture interference-plus-noise effects. If NM is sufficiently large, the interference can be assumed to be Gaussian with variance

$$\begin{aligned} \bar{\sigma}_{j,\ell}^2(k) &:= \text{var} \left\{ \sum_{\substack{\ell'=1 \\ \ell' \neq \ell}}^{NM} g_{j,\ell\ell'}(k) s_{\ell'} + w_{j,\ell}(k) \right\} \\ &= \sum_{\substack{\ell'=1 \\ \ell' \neq \ell}}^{NM} g_{j,\ell\ell'}^2(k) \sigma_s^2 + \Sigma_{j,\ell\ell}(k) \end{aligned} \quad (16)$$

where $\Sigma_{j,\ell\ell}(k)$ is the (ℓ, ℓ) -th entry of $\Sigma_j(k)$. Using (16), the SNR in (15) becomes

$$\rho_{j,\ell}(k) = E\{[g_{j,\ell\ell}(k) s_\ell]^2\} / \bar{\sigma}_{j,\ell}^2(k) = g_{j,\ell\ell}^2(k) \sigma_s^2 / \bar{\sigma}_{j,\ell}^2(k). \quad (17)$$

Based on (17), the symbol error rate (SER) can be readily obtained in closed form, or, it can be bounded as in e.g., [12, Sec. 4.3] for popular one- or two-dimensional QAM constellation points $s_\ell \in \mathcal{A}$ transmitted over an AWGN channel with SNR $\rho_{j,\ell}(k)$. As an example, if s_ℓ is drawn from a q -ary PAM constellation, the optimal SER per sensor j at iteration k is given by

$$P_{e,\ell}^j(k) = 2 \left(1 - \frac{1}{q}\right) Q \left(\sqrt{\frac{3}{q^2 - 1}} \rho_{j,\ell}(k) \right) \quad (18)$$

where $Q(x) := (1/\sqrt{2\pi}) \int_x^\infty \exp(-t^2/2) dt$ denotes the Gaussian tail function.

Such SER expressions can be easily obtained also when inter-sensor links are corrupted by zero-mean additive noise. Because the iterations are linear, the iterates $\mathbf{s}_j(k)$ in (12) will now include an extra colored noise term with covariance determined by the inter-sensor noise level and the network topology. To obtain the SNR in this case, it suffices to incorporate this extra noise term into $\mathbf{w}_j(k)$, update the variance term $\bar{\sigma}_{j,\ell}^2$ in (16), and plug it into (17).

IV. DISTRIBUTED CONSENSUS ON SUFFICIENT STATISTICS

An alternative approach to solving (3) in a distributed fashion is to have all sensors agree on minimal sufficient statistics for the demodulation problem. The motivation behind this approach is twofold: i) reduce the communication overhead per sensor for a prescribed target SER; and ii) allow for more general (possibly non-linear) (near-) optimal demodulators.

Bearing these goals in mind, the ML demodulator in (3) can be re-expressed as

$$\hat{\mathbf{s}}_{ML} = \arg \max_{\mathbf{s} \in \mathcal{A}^{NM}} \left\{ 2 \left(\sum_{j=1}^J \mathbf{H}_j^T \mathbf{y}_j \right)^T \mathbf{s} - \mathbf{s}^T \left(\sum_{j=1}^J \mathbf{H}_j^T \mathbf{H}_j \right) \mathbf{s} \right\}. \quad (19)$$

Upon defining the sample cross-covariance between the received block \mathbf{y}_j and the channel \mathbf{H}_j as $\boldsymbol{\varphi}_j := \mathbf{H}_j^T \mathbf{y}_j$, and the channel's sample covariance matrix as $\boldsymbol{\Gamma}_j := \mathbf{H}_j^T \mathbf{H}_j$, the ML demodulator in (19) is equivalent to

$$\hat{\mathbf{s}}_{ML} = \arg \max_{\mathbf{s} \in \mathcal{A}^{NM}} \left\{ 2 \left(\frac{1}{J} \sum_{j=1}^J \boldsymbol{\varphi}_j \right)^T \mathbf{s} - \mathbf{s}^T \left(\frac{1}{J} \sum_{j=1}^J \boldsymbol{\Gamma}_j \right) \mathbf{s} \right\}. \quad (20)$$

Thus, in order to solve (20) locally, it suffices for each sensor to acquire the following averages:

$$\bar{\boldsymbol{\varphi}} := \frac{1}{J} \sum_{j=1}^J \boldsymbol{\varphi}_j, \quad \text{and} \quad \bar{\boldsymbol{\Gamma}} := \frac{1}{J} \sum_{j=1}^J \boldsymbol{\Gamma}_j. \quad (21)$$

Given $\bar{\boldsymbol{\varphi}}$ and $\bar{\boldsymbol{\Gamma}}$, the optimal $\hat{\mathbf{s}}_{ML}$ in (20) depends only on the symbol constellation \mathcal{A} , that is assumed available at all sensors. The main insight is summarized in the following proposition:

Proposition 2. (Sufficient statistics for demodulation) *In order to solve the ML demodulation problem (3), it suffices for all sensors to consent on $\bar{\boldsymbol{\varphi}}$ and $\bar{\boldsymbol{\Gamma}}$ in (21), which are known to constitute minimal sufficient statistics for the centralized demodulator in (3).*

The averages $\bar{\boldsymbol{\varphi}}$ and $\bar{\boldsymbol{\Gamma}}$ are also sufficient statistics for sub-optimal (non-ML) and (near-) optimal demodulation algorithms, including the:

- *Distributed ZF and MMSE demodulators*, which from (4) and (5) take the form

$$\hat{\mathbf{s}}_{ZF} = \bar{\boldsymbol{\Gamma}}^{-1} \bar{\boldsymbol{\varphi}} \quad (22)$$

$$\hat{\mathbf{s}}_{MMSE} = \left(\bar{\boldsymbol{\Gamma}} + \frac{1}{J\sigma_s^2} \mathbf{I}_{NM} \right)^{-1} \bar{\boldsymbol{\varphi}}. \quad (23)$$

- *Distributed sphere decoder (SD)*, which uses the fact that $\bar{\boldsymbol{\Gamma}}$ is symmetric positive definite, and thus admits a Cholesky decomposition of the form $\bar{\boldsymbol{\Gamma}} = \mathbf{R}\mathbf{R}^T$ [5, Ch. 4.3]. Based on the latter, the ML demodulator in (20) can be re-expressed as

$$\begin{aligned} \hat{\mathbf{s}}_{ML} &= \arg \max_{\mathbf{s} \in \mathcal{A}^{NM}} \left\{ 2 \bar{\boldsymbol{\varphi}}^T \mathbf{R}^{-1} \mathbf{R} \mathbf{s} - \mathbf{s}^T \mathbf{R}^T \mathbf{R} \mathbf{s} \right. \\ &\quad \left. - \bar{\boldsymbol{\varphi}}^T \mathbf{R}^{-1} (\mathbf{R}^{-1})^T \bar{\boldsymbol{\varphi}} \right\} \\ &= \arg \max_{\mathbf{s} \in \mathcal{A}^{NM}} \left\{ -\|\tilde{\mathbf{y}} - \mathbf{R} \mathbf{s}\|^2 \right\} \end{aligned} \quad (24)$$

where $\tilde{\mathbf{y}} := (\mathbf{R}^{-1})^T \bar{\boldsymbol{\varphi}}$ can be viewed as the vector received over the equivalent channel matrix \mathbf{R} . Note that the objective of demodulating \mathbf{s} in (24) coincides with that of (20). Hence, the SD algorithm can be applied in a distributed fashion too, provided that each sensor j acquires the sufficient statistics $\bar{\boldsymbol{\varphi}}$ and $\bar{\boldsymbol{\Gamma}}$.

Following similar arguments, other demodulation algorithms such as decision-feedback [12, Ch. 10.3], or semi-definite relaxation [16] whose objective function is expressible in terms of (cross-) covariance matrices, can also be written in terms of $\bar{\boldsymbol{\gamma}}$ and $\bar{\boldsymbol{\varphi}}$.

It is worth stressing at this point that if each sensor relies only on local linear ZF or MMSE equalization without cooperation, the demodulation performance will degrade severely. In lieu of cooperation, it is even impossible to employ SD per sensor as in (3). Instead, sensors could employ ML or generalized SD, but still their performance would be poor. On the other hand, the equivalent channel seen by cooperating sensors is generally full rank (so long as $J \geq M$), and the demodulation performance improves considerably, as it will be verified also by the simulations of the next section.

The remaining task is to derive algorithms that reach consensus on each entry of $\bar{\boldsymbol{\Gamma}}$ and $\bar{\boldsymbol{\varphi}}$ in a distributed fashion. This is the theme of the ensuing subsection.

A. Consensus Averaging Algorithms

The averages $\bar{\varphi}$ and $\bar{\Gamma}$ can be found in a distributed fashion by applying the CA algorithm of e.g., [18] per entry. However, when inter-sensor links suffer from noise these algorithms experience slow convergence. For this reason, we will use a CA variant based on the MoM (CA-MoM), in which the average value is found iteratively as the solution of a distributed optimization problem [19]. In either CA or CA-MoM, if the algorithm stops before finding the exact sufficient statistics for (3), each sensor will be allowed to demodulate the signal using the information collected up to that point.

To simplify notation, the scalar variable x_j will be used to denote any entry of φ_j or Γ_j we wish to consent on at sensor j . The k -th iterate at sensor j will be denoted as $\bar{x}_j(k)$. When consensus is achieved, $\lim_{k \rightarrow \infty} \bar{x}_j(k) = \bar{x} := (1/J) \sum_{j=1}^J x_j$, which is equal to the corresponding entry in $\bar{\varphi}$ or $\bar{\Gamma}$ (cf. (21)).

The CA-MoM approach originates from the well-known fact that the sample average can be viewed as the solution of an LS cost, namely $\bar{x} = \arg \min_{\theta} \frac{1}{2} \sum_{j=1}^J (x_j - \theta)^2 = \arg \min_{\theta} \frac{1}{2} \|\mathbf{x} - \mathbf{1}_J \theta\|^2$. The CA-MoM iterations for this problem are given by

$$v_{ji}(k) = v_{ji}(k-1) + \frac{\alpha}{2} (\bar{x}_j(k) - \bar{x}_i(k)), \quad j \in \mathcal{J}, i \in \mathcal{N}_j \quad (25a)$$

$$\bar{x}_j(k+1) = \frac{1}{1 + 2\alpha|\mathcal{N}_j|} \left\{ x_j - \sum_{i \in \mathcal{N}_j} [v_{ji}(k) - v_{ij}(k) - \alpha(\bar{x}_j(k) + \bar{x}_i(k))] \right\}, \quad j \in \mathcal{J} \quad (25b)$$

for any $\alpha > 0$. Indeed, upon setting $\mathbf{H} = \mathbf{1}$ and substituting \mathbf{y}_j for x_j , the DC-DS iterations (10a)-(10b) boil down to (25a)-(25b). The iterates in (25a)-(25b) are provably convergent under noisy or random failing inter-sensor links [19].

Remark 4. (*Communication savings*) Recalling that $\mathbf{H}_j := \mathbf{I}_N \otimes \mathbf{h}_j^T$, and due to the fact that Γ_j is symmetric, the problem of consenting on each entry of the $NM \times NM$ matrix can be reduced to consenting on $M(M+1)/2$ scalar entries. Thus, including φ_j , the overall number of scalars required to consent on is $NM + M(M+1)/2$, which is quadratic in M and linear in N but not dependent on the number of hypotheses $|\mathcal{A}|^{NM}$.

As for the computational complexity, after consenting on the sufficient statistics, each sensor can solve not only centralized ML demodulation problems incurring exponential complexity, but also sub-optimal (e.g., ZF/MMSE ones) with linear complexity, or, (near-) optimal ones (e.g., SD) with polynomial complexity on the average [4, Ch. 5].

B. Performance analysis

This section derives bounds for the SER performance of the DC-SS algorithm as a function of the number of iterations k , even before consensus on the *exact* (cross-) covariance is achieved. We will first focus on the ML detector to benchmark the (near-) ML solution provided by the SD in (20). Subsequently, we will consider the performance of the simpler ZF and MMSE demodulators in (22) and (23), respectively.

1) *Pairwise error probability bound for distributed ML demodulation.* Invoking the union bound, the error probability

of the ML demodulator in (3) conditioned on the channel, namely $P_{e|h}$, can be bounded by the pairwise error probability (PEP), which is the probability of erroneously detecting \mathbf{s} as $\mathbf{s}' \in \mathcal{A}^{NM}$ with $\mathbf{s}' \neq \mathbf{s}$. Since PEP captures the probability of block errors, and one block error is caused by at least one symbol error, it follows that the PEP upper-bounds the SER. Letting $P_{\mathbf{s} \rightarrow \mathbf{s}'|h}^j(k)$ denote the conditional PEP at sensor j and iteration k , it holds that $P_{e|h}^j(k) \leq \sum_{\mathbf{s} \in \mathcal{A}^{NM}} P_{\mathbf{s}} \sum_{\mathbf{s}' \neq \mathbf{s}} P_{\mathbf{s} \rightarrow \mathbf{s}'|h}^j(k)$, where $P_{\mathbf{s}}$ is the probability of transmitting \mathbf{s} . Given $\bar{\varphi}_j(k)$ and $\bar{\Gamma}_j(k)$ per sensor j at iteration k , the local ML estimate of \mathbf{s} , namely $\hat{\mathbf{s}}_j(k)$, becomes

$$\hat{\mathbf{s}}_j(k) = \arg \max_{\mathbf{s} \in \mathcal{A}^{NM}} \{ 2\bar{\varphi}_j^T(k)\mathbf{s} - \mathbf{s}^T \bar{\Gamma}_j(k) \mathbf{s} \}. \quad (26)$$

The PEP for the symbols detected as in (26) is clearly

$$P_{\mathbf{s} \rightarrow \mathbf{s}'|h}^j(k) = \Pr \left[2\bar{\varphi}_j^T(k)\mathbf{s} - \mathbf{s}^T \bar{\Gamma}_j(k) \mathbf{s} < 2\bar{\varphi}_j^T(k)\mathbf{s}' - \mathbf{s}'^T \bar{\Gamma}_j(k) \mathbf{s}' \right]. \quad (27)$$

Using Lemma 1, the running averages can be expressed as

$$\bar{\varphi}_j(k) = \frac{1}{J} \sum_{i=1}^J c_{ij}(k) \varphi_i, \quad \text{and} \quad \bar{\Gamma}_j(k) := \frac{1}{J} \sum_{i=1}^J c_{ij}(k) \Gamma_i \quad (28)$$

where the weights $c_{ij}(k)$ are uniquely characterized by the network topology and by the coefficient α in (25a)-(25b). In the limit, it holds that $\lim_{k \rightarrow \infty} c_{ij}(k) = 1$. Based on (28) and after substituting $\varphi_i = \mathbf{H}_i^T \mathbf{H}_i \mathbf{s} + \mathbf{H}_i^T \boldsymbol{\epsilon}_i$ into (27), we find

$$P_{\mathbf{s} \rightarrow \mathbf{s}'|h}^j(k) = \Pr \left[(\mathbf{s} - \mathbf{s}')^T \bar{\Gamma}_j(k) (\mathbf{s} - \mathbf{s}') - 2 \left(\frac{1}{J} \sum_{i=1}^J c_{ij}(k) \mathbf{H}_i^T \boldsymbol{\epsilon}_i \right)^T (\mathbf{s} - \mathbf{s}') < 0 \right] = Q \left(\frac{(\mathbf{s} - \mathbf{s}')^T \bar{\Gamma}_j(k) (\mathbf{s} - \mathbf{s}')}{\sqrt{2(\mathbf{s} - \mathbf{s}')^T \tilde{\Gamma}_j(k) (\mathbf{s} - \mathbf{s}')}} \right) \quad (29)$$

where $\tilde{\Gamma}_j(k) := (1/J^2) \sum_{i=1}^J c_{ij}^2(k) \Gamma_i$, and the second equality follows from the Gaussianity of $\boldsymbol{\epsilon}_i$. Notice that when consensus is achieved, $c_{ij}(k) = 1$ and so $\tilde{\Gamma}_j(k) = (1/J) \bar{\Gamma}$. In this case, the PEP becomes

$$\lim_{k \rightarrow \infty} P_{\mathbf{s} \rightarrow \mathbf{s}'|h}^j(k) = Q \left(\sqrt{\frac{1}{2} (\mathbf{s} - \mathbf{s}')^T \left(\sum_{j=1}^J \mathbf{H}_j^T \mathbf{H}_j \right) (\mathbf{s} - \mathbf{s}')} \right) \quad (30)$$

which equals the PEP obtained by the centralized demodulator in (3); see e.g., [4, Ch. 2]. In other words, PEP performance of distributed demodulation can be rendered asymptotically equivalent to the one corresponding to a multiple-input multiple-output (MIMO) system with M transmit antennas and J receive antennas [4, Ch. 2].

A relevant performance measure is the *diversity* order achieved by each sensor j at any given iteration k , defined as [4, Ch. 2.6]

$$G_d^j(k) = \lim_{\sigma_h^2 \rightarrow \infty} \frac{\log E_h \{ P_{e|h}^j(k) \}}{\log(\sigma_s^2 \sigma_h^2)} \quad (31)$$

where σ_h^2 is the variance of the channel coefficients. Interestingly, it is not necessary to let $k \rightarrow \infty$ to achieve the diversity

of the centralized system distributedly, as established in the following proposition.

Proposition 3. (Diversity order after a finite number of iterations) *The distributed ML demodulator in (26) achieves the same diversity order as the centralized ML of (3) in a finite number of iterations.*

Proof: See Appendix C for the proof. ■

Intuitively, after a number of iterations, $\bar{\Gamma}_j(k)$ achieves the same rank as $\bar{\Gamma}$. Because the diversity order is characterized by the rank of $\bar{\Gamma}$ [4, Ch. 2], both systems achieve the same diversity order.

We will wrap up the performance analysis of our distributed ML demodulator by considering noisy inter-sensor links. In this case, $\hat{\varphi}_j(k)$ and $\hat{\Gamma}_j(k)$ can be written as $\hat{\varphi}_j(k) = \bar{\varphi}_j(k) + \boldsymbol{\eta}_j(k)$ and $\hat{\Gamma}_j(k) = \bar{\Gamma}_j(k) + \boldsymbol{\Xi}_j(k)$, where $\bar{\varphi}_j(k)$ and $\bar{\Gamma}_j(k)$ are defined in (28), $\boldsymbol{\eta}_j(k) \sim \mathcal{CN}(\mathbf{0}, \mathbf{I}_N \sigma_j^2(k))$, and $\text{vec}(\boldsymbol{\Xi}_j(k)) \sim \mathcal{CN}(\mathbf{0}, \mathbf{I}_{N^2 M^2} \sigma_j^2(k))$ with $\sigma_j(k)$ bounded. Notice that consensus is carried on a per-entry basis and the noise terms $\boldsymbol{\eta}_j(k)$ and $\boldsymbol{\Xi}_j(k)$ are uncorrelated across entries. Therefore, the PEP now becomes [cf. (29)]

$$\begin{aligned} & P_{\mathbf{s} \rightarrow \mathbf{s}' | h}^j(k) \\ &= \Pr \left[(\mathbf{s} - \mathbf{s}')^T \bar{\Gamma}_j(k) (\mathbf{s} - \mathbf{s}') + \mathbf{s}^T \boldsymbol{\Xi}_j(k) \mathbf{s} - (\mathbf{s}')^T \boldsymbol{\Xi}_j(k) \mathbf{s}' \right. \\ & \quad \left. - 2\boldsymbol{\eta}_j^T(k) (\mathbf{s} - \mathbf{s}') - 2 \left(\frac{1}{J} \sum_{i=1}^J c_{ij}(k) \mathbf{H}_i^T \boldsymbol{\epsilon}_i \right)^T (\mathbf{s} - \mathbf{s}') < 0 \right] \\ &= Q \left(\frac{(\mathbf{s} - \mathbf{s}')^T \bar{\Gamma}_j(k) (\mathbf{s} - \mathbf{s}')}{\sqrt{2(\mathbf{s} - \mathbf{s}')^T [\tilde{\Gamma}_j(k) + \mathbf{I}_{NN} \sigma_j^2(k)] (\mathbf{s} - \mathbf{s}') + \sigma_{\boldsymbol{\Xi}}^2(k)}} \right) \end{aligned} \quad (32)$$

where $\sigma_{\boldsymbol{\Xi}}^2(k) := \text{var} \{ \mathbf{s}^T \boldsymbol{\Xi}_j(k) \mathbf{s} - (\mathbf{s}')^T \boldsymbol{\Xi}_j(k) \mathbf{s}' \}$. Because the denominator in (32) is strictly larger than that of (29), the overall system performance is worse when compared to the noise-free case. As expected, the presence of noise in inter-sensor communications reduces the equivalent overall SNR. As a sanity check, observe that when $\sigma_j^2(k) \rightarrow 0$, equation (32) reduces to (27). Because diversity is defined as σ_h^2 goes to infinity, $\sigma_j^2(k)$ will vanish and both systems with and without inter-sensor noise will achieve the same diversity order. This argument can be made rigorous, albeit after employing tedious manipulations. Furthermore, using the same logic as in Appendix C, it is not difficult to deduce that full diversity is likewise achievable after a finite number of iterations even for non-ideal inter-sensor links.

2) *Linear demodulation.* Consider the distributed ZF demodulator in (22). Substituting $\bar{\Gamma}$ and $\bar{\varphi}$ for $\bar{\Gamma}_j(k)$ and $\bar{\varphi}_j(k)$, the estimate $\mathbf{s}_j(k)$ of $\hat{\mathbf{s}}_{ZF}$ at sensor j and iteration k is given by

$$\mathbf{s}_j(k) = \bar{\Gamma}_j(k)^{-1} \bar{\varphi}_j(k) = \frac{1}{J} \sum_{i=1}^J c_{ij}(k) \bar{\Gamma}_j^{-1}(k) \boldsymbol{\varphi}_i \quad (33)$$

where the second inequality comes from (28). Since $\boldsymbol{\varphi}_i = \mathbf{H}_i^T \mathbf{H}_i \mathbf{s} + \mathbf{H}_i^T \boldsymbol{\epsilon}_i$, it follows that

$$\mathbf{s}_j(k) = \tilde{\mathbf{G}}_j(k) \mathbf{s} + \tilde{\mathbf{w}}_j(k) \quad (34)$$

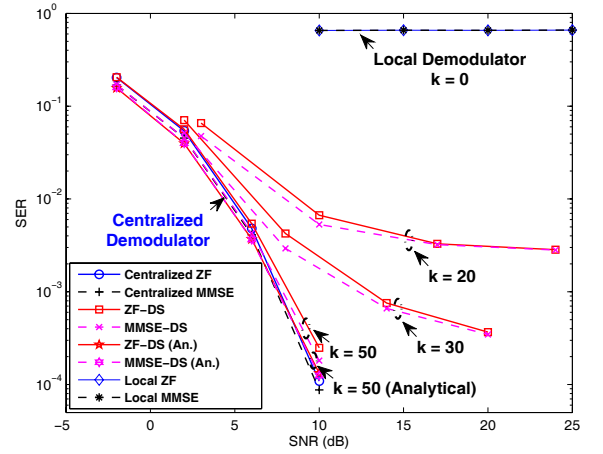


Fig. 2. SER vs. SNR (in dB) curves for the DC-DS algorithm with $M = 4$, $N = 2$, 4-PAM, and ideal inter-sensor links. Local and centralized demodulators are also included for comparison.

where now $\tilde{\mathbf{G}}_j(k) := (1/J) \sum_{i=1}^J c_{ij}(k) \bar{\Gamma}_j^{-1}(k) \mathbf{H}_i^T \mathbf{H}_i$ and $\tilde{\mathbf{w}}_j(k) := (1/J) \sum_{i=1}^J c_{ij}(k) \bar{\Gamma}_j^{-1}(k) \mathbf{H}_i^T \boldsymbol{\epsilon}_i$. The rest of the steps are identical to those in Section III-B: (i) write the ℓ -th entry of $\mathbf{s}_j(k)$ as in (15); (ii) find the variance of the interference-plus-noise term in (16); and (iii) formulate an equivalent SNR for the ℓ -th entry of $\mathbf{s}_j(k)$ as in (17). Recall also that similar performance results can be obtained for the MMSE demodulator by substituting $\bar{\Gamma}_j^{-1}(k)$ for $(\bar{\Gamma}_j(k) + \frac{1}{J} \mathbf{I}_{NM})^{-1}$ in (33). Performance analysis in the presence of inter-sensor noise is far more challenging in this case, since it involves computing expectations over inverted Gaussian matrices. For this reason, our performance analysis in the presence of noise will rely on simulations.

V. SIMULATIONS

The distributed demodulators of Sections III and IV are tested and compared in this section. The WSN has $J = 10$ sensors uniformly placed over the unit square. The communication range of each sensor is $r = 0.5$. Two nodes are connected if their Euclidean distance is less than r . As a result, the number of graph edges here is $|\mathcal{E}| = 18$. Symbols are drawn from a 4-PAM constellation and directly mapped to the entries of matrix \mathbf{S} . The AP has $M = 4$ antennas, and the block duration is $N = 2$ time slots. The channels $\mathbf{h}_j \sim \mathcal{N}(\mathbf{0}_M, \sigma_h^2 \mathbf{I}_M)$ are independently and identically distributed. The average AP-sensor SNR in dB is $SNR := 10 \log_{10}(\sigma_s^2 \sigma_h^2)$.

Test Case 1 (Distributed linear demodulators). In this case, the average SER of the DC-DS in Section III is simulated for ideal and non-ideal inter-sensor communication links. Both distributed ZF and MMSE demodulators based on the DC-DS iterations (10a)-(10b) are considered (tagged as ZF-DS and MMSE-DS, respectively). Each sensor j quantizes the iterate $\mathbf{s}_j(k)$ to obtain the demodulation result at iteration k .

Fig. 2 plots SER as a function of the AP-to-sensor SNR assuming ideal inter-sensor links for different values of the iteration index k . The centralized ZF and MMSE demodulators (using \mathbf{y} and \mathbf{H} in (4) and (5)) are included as

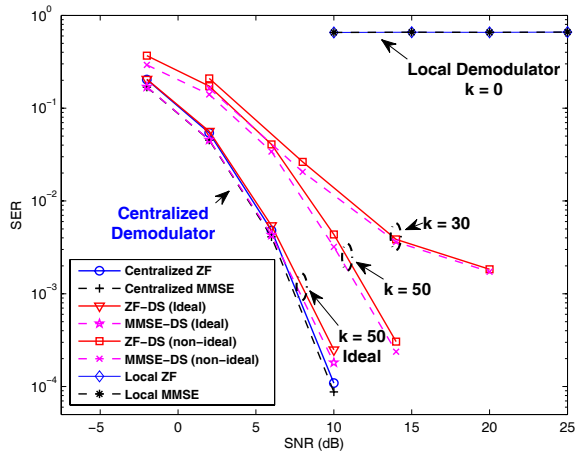


Fig. 3. SER vs. SNR (in dB) curves for the DC-DS algorithm with $M = 4$, $N = 2$, 4-PAM, and non-ideal inter-sensor links. Local and centralized demodulators are also included for comparison.

a benchmark. The *local* demodulators using only y_j and \mathbf{H}_j are provided by the distributed initialization at iteration number $k = 0$. The analytical SER obtained as detailed in (18) is also included. Clearly, the average SER improves as the number of iterations increases, approaching that of the centralized benchmark after approximately 50 iterations of the ZF-DS and MMSE-DS demodulators. In the centralized setting, the MMSE is known to outperform the ZF, but their diversity orders are the same. This is also observed for the distributed setting after a finite number of iterations. Notice that local demodulators perform poorly. This is because each sensor locally faces an under-determined scenario (the number of transmit antennas is larger than the number of receive antennas). As the number of consensus iterations increases, the *equivalent* number of receive antennas increases and the system becomes identifiable.

Fig. 3 depicts the error performance when considering non-ideal inter-sensor links. Single-hop exchanges are corrupted by AWGN at equivalent $SNR' = SNR + 10\text{dB}$. Also, links are assumed to fail independently with probability (w.p.) 0.1. The noise-free (ideal) case from Fig. 2 after $k = 50$ iterations is also included here for comparison. Clearly, non-ideal inter-sensor links degrade the error performance. Notwithstanding this performance loss, the slope of the SER curve for both ideal and non-ideal cases is the same; i.e., the same diversity order is obtained in both cases.

Test Case 2 (Distributed demodulation using consensus on sufficient statistics). Here, the performance of the algorithm based on the DC-SS approach of Section IV is simulated. As discussed in Section IV, this approach allows for a broader class of demodulation methods. Distributed SD and ZF (tagged as ZF-SS) are tested by consenting on sufficient statistics through iterations (25a)-(25b). After a given number of iterations k , each sensor relies on the averages $\bar{\Gamma}(k)$ and $\bar{\varphi}(k)$ collected up to that instant to run the demodulators using either (22) or (20). Fig. 4 plots the resulting SER vs. SNR curves under ideal inter-sensor links for the SD and the ZF-SS demodulators. Analytical results obtained in Section IV-B for ZF-SS are also included. The average SER

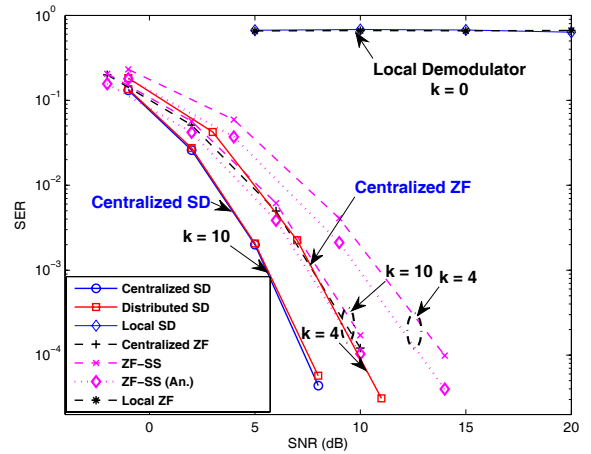


Fig. 4. SER vs. SNR (in dB) curves for the DC-SS algorithm with $M = 4$, $N = 2$, 4-PAM, and ideal inter-sensor links. Local and centralized demodulators are also included for comparison.

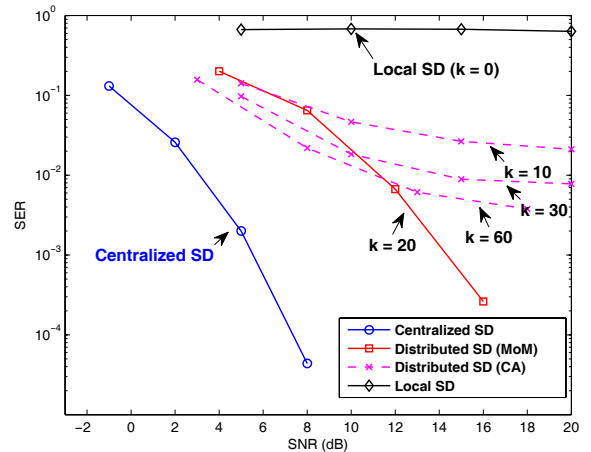


Fig. 5. SER vs. SNR (in dB) curves for the DC-SS algorithm with $M = 4$, $N = 2$, 4-PAM, and non-ideal inter-sensor links. Local and centralized demodulators are also included for comparison.

improves as the number of iterations increases much more rapidly compared to Fig. 2, approaching that of the centralized benchmark after about $k = 10$ iterations. (See Test Case 3 for more detailed comparisons.) This is not surprising since the diversity collected by the demodulator increases as statistical information from neighboring sensors becomes available as iterations proceed. Fig. 5 shows the performance of distributed SD when imperfect inter-sensor links are present, where now the inter-sensor $SNR' = SNR + 15\text{dB}$ and links fail w.p. 0.1, as before. For comparison, the CA algorithm with the vanishing step size proposed in [6] to cope with noise is also implemented. The resulting SER of both algorithms degrades w.r.t. the one in Fig. 4, as expected. As discussed in Section IV-B, even under non-ideal links, the CA-MoM algorithm after $k = 20$ iterations exhibits approximately the same diversity as the centralized SD. However, the larger the iteration number k is, the slower the CA iterations progress, especially at high SNR.

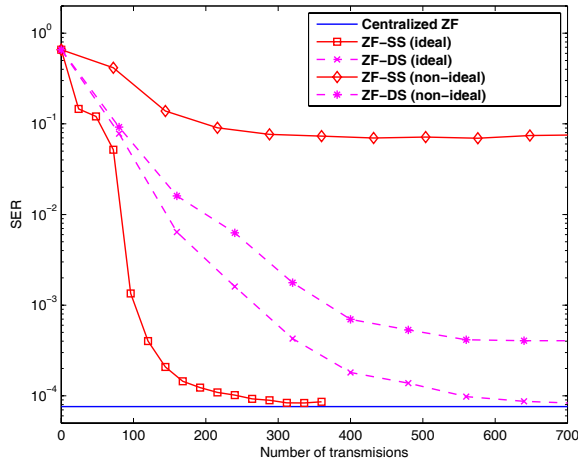


Fig. 6. SER vs. number of transmissions for the distributed ZF demodulators under both ideal and non-ideal inter-sensor links with $M = 4$, $N = 2$ and 4-PAM.

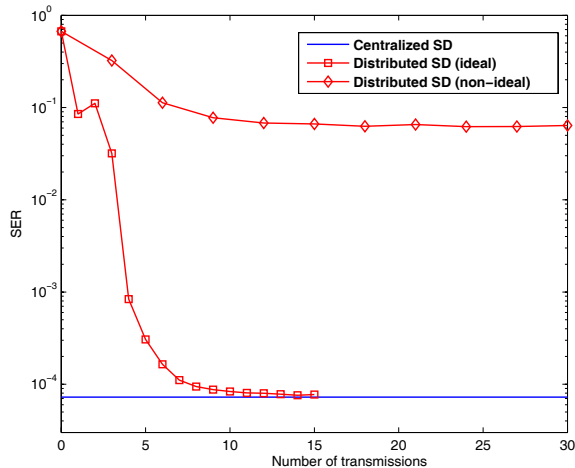


Fig. 7. SER vs. number of transmissions for the distributed SD demodulator using consensus on sufficient statistics under both ideal and non-ideal inter-sensor links with $M = 4$, $N = 2$ and 4-PAM.

Test Case 3 (Performance comparisons). Here, we compare the DC-DS and DC-SS demodulators of Sections III and IV. The key to comparing both algorithms is to find the SER for the same number of transmissions (that might be different from the number of iterations of the algorithm). At each iteration of the DC-DS, the number of transmissions is proportional to $NM = 8$, which is the length of $\hat{\mathbf{s}}_j(k)$; while the number of transmissions for DC-SS is proportional to $NM + M(M + 1)/2 = 18$, as pointed out in Remark 4. We set $SNR = 10$ dB, and for the non-ideal inter-sensor links $SNR' = 25$ dB with link failure probability equal to 0.1. Fig. 6 compares the average SER of both ZF-DS and ZF-SS algorithms as a function of the number of transmissions. For ideal inter-sensor links, the ZF-SS algorithm exhibits fast convergence to the centralized benchmark. However, under non-ideal inter-sensor links, its performance degrades considerably. The ZF-DS algorithm exhibits slower convergence

rate compared to the ZF-SS, but it is more robust to non-ideal links. Fig. 7 plots the average SER of the SD algorithm. Clearly, the distributed SD algorithm converges faster than either ZF-DS or ZF-SS under ideal links at the price of increased demodulation complexity. If links are non-ideal, however, its performance also degrades severely. Finally, note that the distributed SD algorithm involves nonlinear operations (Cholesky decomposition) over the CA-MoM iterates in (25a)-(25b), which explains the non-monotonic behavior in Fig. 7.

VI. CONCLUDING SUMMARY

Distributed demodulation of symbols transmitted from a multi-antenna AP to a wireless sensor network was investigated. Two iterative algorithms were developed to obtain distributed estimates of the AP's transmitted symbols. The DC-DS one resulted after viewing the linear demodulation task as an unconstrained optimization problem solved with the MoM to obtain the optimal solution in a distributed fashion. For ML optimal demodulation and various sub-optimal alternatives, the DC-SS scheme aimed at consensus on the average local (cross-) covariance terms, which are sufficient statistics for the general ML, SD and ZF/MMSE demodulation problems. Both DC-DS and DC-SS algorithms entail affordable communication complexity, irrespective of the constellation size. The per-iteration error performance was analyzed for both algorithms, and the number of iterations needed to attain a prescribed error rate was quantified. Simulations suggest that for ideal inter-sensor links, consenting on sufficient statistics offers faster convergence and more flexibility to choose from a variety of demodulation options including ML, near-ML, and sub-optimum linear algorithms. However, under non-ideal inter-sensor links, the performance of nonlinear demodulators degrades considerably as the SNR drops. In this case, consenting on the demodulated symbols, although limited to linear receivers, is a more suitable approach.

APPENDIX A

DERIVATION OF (10a)-(10b)

The k -th iteration of the MoM solver of (9) is [1, pg. 255]

$$\mathbf{s}(k+1) = \arg \min_{\mathbf{s}} \mathcal{L}_a(\mathbf{s}, \mathbf{z}(k), \mathbf{v}(k), \mathbf{v}'(k)) \quad (35a)$$

$$\mathbf{z}(k+1) = \arg \min_{\mathbf{z} \in \mathcal{C}_z} \mathcal{L}_a(\mathbf{s}(k+1), \mathbf{z}, \mathbf{v}(k), \mathbf{v}'(k)) \quad (36a)$$

$$\mathbf{v}_{ji}(k+1) = \mathbf{v}_{ji}(k) + \alpha(\mathbf{s}_j(k+1) - \mathbf{z}_{ji}(k+1)), \quad j \in \mathcal{J}, i \in \mathcal{N}_j \quad (36b)$$

$$\mathbf{v}'_{ji}(k+1) = \mathbf{v}'_{ji}(k) + \alpha(-\mathbf{s}_i(k+1) - \mathbf{z}'_{ji}(k+1)), \quad j \in \mathcal{J}, i \in \mathcal{N}_j \quad (36c)$$

Because the variables \mathbf{s}_j in (9) are not coupled, (35a) is equivalent to the following J separable sub-problems, one per sensor j

$$\mathbf{s}_j(k+1) = \arg \min_{\mathbf{s}_j} \left\{ \frac{1}{2} \|\mathbf{y}_j - \mathbf{H}_j \mathbf{s}_j\|^2 + \sum_{i \in \mathcal{N}_j} (\mathbf{v}_{ji}(k) - \mathbf{v}'_{ij}(k))^T \mathbf{s}_j + \sum_{i \in \mathcal{N}_j} \frac{\alpha}{2} \{ \|\mathbf{s}_j - \mathbf{z}_{ji}(k)\|^2 + \|\mathbf{s}_j - \mathbf{z}'_{ij}(k)\|^2 \} \right\}. \quad (37)$$

Being linear-quadratic in \mathbf{s}_j , each of these sub-problems can be solved in closed form to obtain

$$\mathbf{s}_j(k+1) = (\mathbf{H}_j^T \mathbf{H}_j + 2\alpha |\mathcal{N}_j| \mathbf{I})^{-1} \left\{ \mathbf{H}_j^T \mathbf{y}_j - \sum_{i \in \mathcal{N}_j} [\mathbf{v}_{ji}(k) - \mathbf{v}'_{ij}(k) - \alpha(\mathbf{z}_{ji}(k) - \mathbf{z}'_{ij}(k))] \right\}. \quad (38)$$

Similarly, $\mathbf{z}(k+1)$ in (36a) is obtained by solving the following $2|\mathcal{E}|$ sub-problems indexed by $(j, i) \in \mathcal{E}$

$$\begin{aligned} & \{\mathbf{z}_{ji}(k+1), \mathbf{z}'_{ji}(k+1)\} \\ &= \arg \min_{\mathbf{z}_{ji} + \mathbf{z}'_{ji} = \mathbf{0}} \left\{ -\mathbf{v}_{ji}^T(k) \mathbf{z}_{ji} - [\mathbf{v}'_{ji}(k)]^T \mathbf{z}'_{ji} \right. \\ & \quad \left. + \frac{\alpha}{2} \|\mathbf{s}_j(k+1) - \mathbf{z}_{ji}\|^2 + \frac{\alpha}{2} \|\mathbf{s}_j(k+1) - \mathbf{z}'_{ji}\|^2 \right\}. \quad (39) \end{aligned}$$

If $\mathbf{v}_{ji}(k)$ and $\mathbf{v}'_{ji}(k)$ are initialized as $\mathbf{v}_{ji}(0) = \mathbf{v}'_{ji}(0) \forall (j, i) \in \mathcal{E}$, the solution to (39) for $k=0$ becomes $\mathbf{z}_{ji}(1) = -\mathbf{z}'_{ji}(1) = \frac{1}{2}(\mathbf{s}_j(1) + \mathbf{s}_i(1))$. Substituting this expression into (36b) and (36c) yields

$$\mathbf{v}_{ji}(1) = \mathbf{v}'_{ji}(1) = \mathbf{v}_{ji}(0) + \frac{\alpha}{2}(\mathbf{s}_j(1) - \mathbf{s}_i(1)). \quad (40)$$

Proceeding by induction, if $\mathbf{v}_{ji}(k) = \mathbf{v}'_{ji}(k)$, the solution to (39) is

$$\mathbf{z}_{ji}(k+1) = -\mathbf{z}'_{ji}(k+1) = \frac{1}{2}(\mathbf{s}_j(k+1) + \mathbf{s}_i(k+1)). \quad (41)$$

Substituting (41) into (36b) and (36c) proves that

$$\mathbf{v}_{ji}(k+1) = \mathbf{v}'_{ji}(k+1) = \mathbf{v}_{ji}(k) + \frac{\alpha}{2}(\mathbf{s}_j(k+1) - \mathbf{s}_i(k+1)) \quad (42)$$

which establishes along with (40) that $\mathbf{v}_{ji}(k) = \mathbf{v}'_{ji}(k) \forall k > 0$.

Equation (42) shows that it is sufficient to update only one set of multipliers $\{\{\mathbf{v}_{ji}(k)\}_{i \in \mathcal{N}_j}\}_{j \in \mathcal{J}}$ per iteration as in (10a). Finally, substituting (41) into (38) proves the validity of (10b).

APPENDIX B PROOF OF LEMMA 1

Substituting (10a) into (10b) leads to

$$\mathbf{s}_j(k+1) = (\mathbf{H}_j^T \mathbf{H}_j + 2\alpha |\mathcal{N}_j| \mathbf{I}_{NM})^{-1} \left\{ \mathbf{H}_j^T \mathbf{y}_j - \sum_{i \in \mathcal{N}_j} [\mathbf{v}_{ji}(k-1) - \mathbf{v}_{ij}(k-1) - 2\alpha \mathbf{s}_i(k)] \right\}. \quad (43)$$

Subtracting (43) from its counterpart written for $\mathbf{s}_j(k)$ leads to the multiplier-free recursion

$$\mathbf{s}_j(k+1) = \mathbf{s}_j(k) + 2\alpha (\mathbf{H}_j^T \mathbf{H}_j + 2\alpha |\mathcal{N}_j| \mathbf{I}_{NM})^{-1} \sum_{i \in \mathcal{N}_j} [\mathbf{s}_i(k) - \mathbf{s}_i(k-1)]. \quad (44)$$

Hence, to show that $\mathbf{s}_j(k) = \mathbf{C}_j(k) \mathbf{y}$, with $\mathbf{C}_j(k) := [\mathbf{C}_{j1}(k), \dots, \mathbf{C}_{jJ}(k)]$, it suffices to establish this linear relationship for $k=1, 2$ and proceed by induction. Wlog initialize (10a)-(10b) with $\mathbf{v}_{ji}(0) = \mathbf{0}_{NM}$, $\forall (j, i) \in \mathcal{E}$, and let $\mathbf{s}_j(1)$ equal the local ZF demodulator, namely

$$\mathbf{s}_j(1) = (\mathbf{H}_j^T \mathbf{H}_j)^\dagger \mathbf{H}_j^T \mathbf{y}_j = \mathbf{C}_{jj}(1) \mathbf{y}_j \quad (45)$$

where $(\cdot)^\dagger$ denotes matrix pseudo-inverse. Clearly $\mathbf{C}_j(1)$ has all zero entries except for the j -th block. Furthermore, for $k=2$ it holds that (cf. (43))

$$\begin{aligned} \mathbf{s}_j(2) &= (\mathbf{H}_j^T \mathbf{H}_j + 2\alpha |\mathcal{N}_j| \mathbf{I}_{NM})^{-1} \left\{ \mathbf{H}_j^T \mathbf{y}_j + 2\alpha \sum_{i \in \mathcal{N}_j} \mathbf{s}_i(1) \right\} \\ &= \mathbf{C}_{jj}(2) \mathbf{y}_j + \sum_{i \in \mathcal{N}_j} \mathbf{C}_{ji}(2) \mathbf{y}_i \quad (46) \end{aligned}$$

where the weights are given by

$$\begin{aligned} \mathbf{C}_{jj}(2) &= (\mathbf{H}_j^T \mathbf{H}_j + 2\alpha |\mathcal{N}_j| \mathbf{I}_{NM})^{-1} \mathbf{H}_j^T \\ \mathbf{C}_{ji}(2) &= 2\alpha (\mathbf{H}_j^T \mathbf{H}_j + 2\alpha |\mathcal{N}_j| \mathbf{I}_{NM})^{-1} \mathbf{C}_{ii}(1) \quad \forall i \in \mathcal{N}_j. \quad (47) \end{aligned}$$

Using (44), it can be readily proved by induction that the linear relationship $\mathbf{s}_j(k) = \mathbf{C}_j(k) \mathbf{y}$ holds for any $k \geq 3$, and the weights can be obtained iteratively as well.

APPENDIX C PROOF OF PROPOSITION 3

We first prove that there exists a finite k' for which $c_{ij}(k) > 0$ for all $k \geq k'$. For that matter, observe that $c_{ij}(k)$ converges exponentially to 1; hence, each entry of $c_{ij}(k)$ obeys $|c_{ij}(k) - 1| \leq C \lambda^k$, $\forall k$, for some $0 < C < \infty$ and $0 < \lambda < 1$ (cf. [19, Appendix E]). Thus, to guarantee that $c_{ij}(k) > 0$, one can choose any k' such that

$$k' \geq \frac{\log C}{\log(1/\lambda)} < \infty. \quad (48)$$

If $c_{ij}(k) > 0 \forall i$, it is possible to bound the PEP in (29) by

$$\begin{aligned} & P_{\mathbf{s} \rightarrow \mathbf{s}'}^j(k) \\ & \leq Q \left(\frac{(\mathbf{s} - \mathbf{s}')^T \left(\sum_{i=1}^J c_{ij}^{\min}(k) \mathbf{H}_i^T \mathbf{H}_i \right) (\mathbf{s} - \mathbf{s}')}{\sqrt{2(\mathbf{s} - \mathbf{s}')^T \left(\sum_{i=1}^J (c_{ij}^{\max}(k))^2 \mathbf{H}_i^T \mathbf{H}_i \right) (\mathbf{s} - \mathbf{s}')}} \right) \\ & \leq Q \left(\kappa_j(k) \sqrt{\frac{1}{2} (\mathbf{s} - \mathbf{s}')^T \left(\sum_{i=1}^J \mathbf{H}_i^T \mathbf{H}_i \right) (\mathbf{s} - \mathbf{s}')} \right) \quad (49) \end{aligned}$$

where $c_{ij}^{\min}(k) := \min_i \{c_{ij}(k)\}$, $c_{ij}^{\max}(k) := \max_i \{c_{ij}(k)\}$ and $\kappa_j(k) := c_{ij}^{\min}(k)/c_{ij}^{\max}(k) \leq 1$. The inequality in (49) implies that the performance of the system is bounded by an equivalent centralized system with SNR reduced by $\kappa_j^2(k)$. Then, the diversity achieved is *at least* the same as the one achieved by the centralized system. On the other hand, the diversity order per local sensor can only be *at most* that of the centralized demodulator. This implies that, so long as $c_{ij}(k) > 0$, (26) achieves the same diversity order as (3).

REFERENCES

- [1] D. P. Bertsekas and J. N. Tsitsiklis, *Parallel and Distributed Computation: Numerical Methods*. Athena Scientific, 1997.
- [2] R. Dabora and S. D. Servetto, "Broadcast channels with cooperating decoders," *IEEE Trans. Inf. Theory*, vol. 52, pp. 5438–5454, Dec. 2006.
- [3] S. C. Draper, B. J. Frey, and F. R. Kschischang, "Interactive decoding of a broadcast message," in *Proc. 41st Allerton Conf. Commun., Contr., Computing*, Oct. 2003.
- [4] G. B. Giannakis, Z. Liu, X. Ma, and S. Zhou, *Space-Time Coding for Broadband Wireless Communications*. John Wiley & Sons, Inc., Jan. 2007.

- [5] G. H. Golub and C. Loan, *Matrix Computations*, 3rd edition. Baltimore, MD: Johns Hopkins University Press, 1996.
- [6] Y. Hatano, A. K. Das, and M. Mesbahi, "Agreement in presence of noise: pseudogradients on random geometric networks," in *Proc. 44th Conf. Decision Control*, Dec. 2005, pp. 6382–6387.
- [7] A. Jadbabaie, J. Lin, and S. Morse, "Coordination of groups of mobile autonomous agents using nearest neighbor rules," *IEEE Trans. Autom. Control*, vol. 48, pp. 988–1001, June 2003.
- [8] S. Kar and J. M. F. Moura, "Consensus based detection in sensor networks: topology optimization under practical constraints," in *Proc. 1st Intl. Wrkshp. Inform. Theory Sensor Networks*, June 2007.
- [9] J. N. Laneman, D. N. C. Tse, and G. W. Wornell, "Cooperative diversity in wireless networks: efficient protocols and outage behavior," *IEEE Trans. Inf. Theory*, vol. 49, pp. 3062–3080, Dec. 2004.
- [10] Y. Liang and G. Kramer, "Rate regions for relay broadcast channels," *IEEE Trans. Inf. Theory*, vol. 53, pp. 3517–3535, Oct. 2007.
- [11] R. Olfati-Saber, E. Frazzoli, E. Franco, and J. S. Shamma, "Belief consensus and distributed hypothesis testing in sensor networks," in *Network Embedded Sensing and Control*, P. J. Antsaklis and P. Tabuada, editors. Springer-Verlag, 2006, pp. 169–182.
- [12] J. G. Proakis and M. Salehi, *Digital Communications*, 5th edition. New York: McGraw-Hill, 2008.
- [13] M. G. Rabbat, R. D. Nowak, and J. A. Bucklew, "Generalized consensus algorithms in networked systems with erasure links," in *Proc. Signal Process. Advances Wireless Commun.*, June 2005.
- [14] V. Saligrama, M. Alanyali, and O. Savas, "Distributed detection in sensor networks with packet losses and finite capacity links," *IEEE Trans. Signal Process.*, vol. 54, pp. 4118–4132, Nov. 2006.
- [15] I. D. Schizas, A. Ribeiro, and G. B. Giannakis, "Consensus in ad hoc WSNs with noisy links—part I: distributed estimation of deterministic signals," *IEEE Trans. Signal Process.*, vol. 56, pp. 350–364, Jan. 2008.
- [16] N. D. Sidiropoulos and Z.-Q. Luo, "A semidefinite relaxation approach to MIMO detection for high-order QAM constellations," *IEEE Signal Process. Lett.*, vol. 13, pp. 525–528, Sep. 2006.
- [17] T. Wang, A. Cano, G. B. Giannakis, and J. Ramos, "Multi-tier cooperative broadcasting with hierarchical modulations," *IEEE Trans. Wireless Commun.*, vol. 6, pp. 3047–3057, Aug. 2007.
- [18] L. Xiao and S. Boyd, "Fast linear iterations for distributed averaging," *System Control Lett.*, vol. 53, pp. 65–78, Sep. 2004.
- [19] H. Zhu, G. B. Giannakis, and A. Cano, "Distributed in-network channel decoding," *IEEE Trans. Signal Process.*, vol. 57, pp. 3970–3983, Oct. 2009.



Her research interests lie in the areas of communication theory and signal processing. Her current research focuses on sparsity-exploiting detection with alphabet constraints and behavior pattern inference for social networks.



Hao Zhu (S'07) received her bachelor's degree from Tsinghua University, Beijing, China in 2006 and the M.Sc. degree from the University of Minnesota, Minneapolis in 2009, both in electrical engineering.

From 2005 to 2006, she worked on radar waveform design as a research assistant with the Intelligent Transportation Information Systems (ITIS) Laboratory, Tsinghua University. Since September 2006, she has been working towards her Ph.D. degree with the Department of Electrical and Computer Engineering at the University of Minnesota.

Alfonso Cano (S'01) received the electrical engineering degree and Ph.D degree with honors in telecommunications engineering from the Universidad Carlos III de Madrid, Madrid, Spain, in 2002 and 2006, respectively. During 2003–2006, he was with the Dept. of Signal Theory and Communications, Universidad Rey Juan Carlos, Madrid, Spain. Since 2007 he has been with the ECE Department at the Univ. of Minnesota, MN, USA, where he is a post-doctoral researcher. His research interests lie in the areas of signal processing and communications.



Georgios B. Giannakis (Fellow'97) received his diploma in electrical engr. from the Ntl. Tech. Univ. of Athens, Greece, 1981. From 1982 to 1986 he was with the Univ. of Southern California (USC), where he received his MSc. in electrical engineering, 1983, MSc. in mathematics, 1986, and Ph.D. in electrical engr., 1986. Since 1999 he has been a professor with the Univ. of Minnesota, where he now holds an ADC Chair in Wireless Telecommunications in the ECE department, and serves as director of the Digital Technology Center.

His general interests span the areas of communications, networking and statistical signal processing - subjects on which he has published more than 285 journal papers, 485 conference papers, 20 book chapters, two edited books, and two research monographs. His current research focuses on compressive sensing, cognitive radios, network coding, cross-layer designs, mobile ad hoc networks, wireless sensor and social networks.

G. B. Giannakis is the (co-)inventor of 15 patents issued, and the (co-)recipient of seven paper awards from the IEEE Signal Processing (SP) and Communications Societies, including the G. Marconi Prize Paper Award in Wireless Communications. He also received Technical Achievement Awards from the SP Society (2000), from EURASIP (2005), a Young Faculty Teaching Award, and the G. W. Taylor Award for Distinguished Research from the University of Minnesota. He is a Fellow of EURASIP, has served the IEEE in a number of posts, including as a Distinguished Lecturer for the IEEE-SP Society.